Impacts of non-canonical El Niño patterns on Atlantic hurricane activity

Sarah Larson,[1] Sang-Ki Lee,[2,3] Chunzai Wang,[3] Eui-Seok Chung,[1] and David Enfield[2,3]

Received 1 June 2012; accepted 27 June 2012; published 28 July 2012.

[1] The impact of non-canonical El Niño patterns, typically characterized by warmer than normal sea surface temperatures (SSTs) in the central tropical Pacific, on Atlantic tropical cyclone (TC) is explored by using composites of key Atlantic TC indices and tropospheric vertical wind shear over the Atlantic main development region (MDR). The highlight of our major findings is that, while the canonical El Niño pattern has a strong suppressing influence on Atlantic TC activity, non-canonical El Niño patterns considered in this study, namely central Pacific warming, El Niño Modoki, positive phase Trans-Niño, and positive phase Pacific meridional mode, all have insubstantial impact on Atlantic TC activity. This result becomes more conclusive when the impact of MDR SST is removed from the Atlantic TC indices and MDR wind shear by using the method of linear regression. Further analysis suggests that the tropical Pacific SST anomalies associated with the non-canonical El Niño patterns are not strong enough to cause a substantial warming of the tropical troposphere in the Atlantic region, which is the key factor that increases the wind shear and atmospheric static stability over the MDR. During the recent decades, the non-canonical El Niños have been more frequent while the canonical El Niño has been less frequent. If such a trend continues in the future, it is expected that the suppressing effect of El Niño on Atlantic TC activity will diminish and thus the MDR SST will play a more important role in controlling Atlantic TC activity in the coming decades. **Citation:** Larson, S., S.-K. Lee, C. Wang, E.-S. Chung, and D. Enfield (2012), Impacts of non-canonical El Niño patterns on Atlantic hurricane activity, *Geophys. Res. Lett.*, *39*, L14706, doi:10.1029/2012GL052595.

1. Introduction

[2] Warm sea surface temperature (SST) anomalies in the tropical Pacific induce a global average warming of the tropical troposphere, via a fast tropical teleconnection mechanism (i.e., Kelvin waves), and thus increase the meridional tropospheric temperature gradient within and across the edge of the tropics [e.g., *Horel and Wallace*, 1981; *Yulaeva and Wallace*, 1994; *Chiang and Sobel*, 2002]. This, in turn, directly increases the vertical wind shear over the Atlantic main development region (MDR, 10°N–20°N and 85°W–15°W), via the thermal wind relationship. Additionally, the teleconnected tropospheric warming over the tropical Atlantic also tends to increase atmospheric static stability and thus causes anomalous diabatic cooling over the MDR [e.g., *Tang and Neelin*, 2004; *Lee et al.*, 2011]. This, in turn, may force the formation of a stationary baroclinic Rossby wave northwest of the MDR, consistent with Gill's simple model of tropical atmospheric circulations, to further increase the MDR wind shear [e.g., *Lee et al.*, 2011]. El Niño events are thus associated with decreased tropical cyclone (TC) activity in the Atlantic basin especially in the deep tropics as a result of increased wind shear and atmospheric static stability over the MDR [e.g., *Gray*, 1984; *Goldenberg and Shapiro*, 1996; *Kossin et al.*, 2010; *Klotzbach*, 2011]. Other environmental factors such as reduced relative humidity also contribute to decreased Atlantic TC activity during El Niño years, as shown in *Camargo et al.* [2007] using a TC genesis index.

[3] The canonical El Niño is characterized by warmer than normal SSTs in the eastern tropical Pacific Ocean. However, El Niño comes in many different flavors – every El Niño event has a somewhat different and distinct character [*Trenberth and Stepaniak*, 2001]. Recently, a newly identified pattern of central equatorial Pacific warming event (non-canonical El Niño hereafter) has received attention due to its increasing frequency in recent decades and its potential link to the influence of anthropogenic global warming [*Yeh et al.*, 2009; *Lee and McPhaden*, 2010]. This non-canonical El Niño is referred to as central Pacific El Niño, El Niño Modoki, warm pool El Niño, Pacific meridional mode and Trans-Niño in the literature [e.g., *Yeh et al.*, 2009; *Ashok et al.*, 2007; *Kao and Yu*, 2009; *Kug et al.*, 2009; *Chiang and Vimont*, 2004; *Trenberth and Stepaniak*, 2001]. It differs from the canonical El Niño in that its warm equatorial SST anomalies are concentrated in the central Pacific with cool SST anomalies flanked in a horseshoe pattern to the east and west [*Ashok et al.*, 2007]. While the canonical El Niño is historically defined as warm SST anomalies in the Niño-3 region (NINO3; 5°S–5°N, 150°W–90°W) or Niño-3.4 region (NINO3.4; 5°S–5°N, 170°W–120°W), several different definitions of the non-canonical El Niño have been referenced in recent literature – central Pacific warming (CPW) [*Yeh et al.*, 2009], El Niño Modoki index (EMI) [*Ashok et al.*, 2007], Pacific meridional mode (PMM) [*Chiang and Vimont*, 2004] and Trans-Niño index (TNI) [*Trenberth and Stepaniak*, 2001]. These definitions were derived to describe the same anomalous central Pacific warming pattern that is captured by the 2nd mode of the empirical orthogonal function analysis of monthly tropical

[1]Rosenstiel School of Marine and Atmospheric Science, University of Miami, Miami, Florida, USA.
[2]Cooperative Institute for Marine and Atmospheric Studies, University of Miami, Miami, Florida, USA.
[3]Atlantic Oceanographic and Meteorological Laboratory, NOAA, Miami, Florida, USA.

Corresponding author: S.-K. Lee, Atlantic Oceanographic and Meteorological Laboratory, NOAA, 4301 Rickenbacker Cswy., Miami, FL 33149, USA. (sang-ki.lee@noaa.gov)

0094-8276/12/2012GL052595

Pacific SST anomalies (EOF2) [*Trenberth and Stepaniak*, 2001; *Ashok et al.*, 2007].

[4] Given a strong dependence of overall Atlantic TC activity on the equatorial Pacific SST anomalies associated with El Niño, there is a clear need for understanding how the response of Atlantic TC activity to non-canonical El Niño differs from that to canonical El Niño. A recent study by *Kim et al.* [2009] suggested that CPW events are associated with a greater-than-average frequency of tropical storms and increasing landfall potential along the Gulf of Mexico coast and Central America. However, *Lee et al.* [2010] performed an independent data analysis to point out that such conclusion could be premature because *Kim et al.* [2009] did not remove in their analysis the local impact of MDR SST, which is as important as the remote impact of tropical Pacific SSTs as shown overwhelmingly in earlier studies [e.g., *Knaff*, 1997; *Knight et al.*, 2006; *Wang et al.*, 2006; *Zhang and Delworth*, 2006; *Vimont and Kossin*, 2007; *Kossin and Vimont*, 2007; *Saunders and Lea*, 2008].

[5] Both *Kim et al.* [2009] and *Lee et al.* [2010] considered only a small number of CPW events to arrive at the contradicting conclusions. Therefore, here, we further attempt to isolate and quantify the impact of non-canonical El Niño on Atlantic TC by using composites of SST, wind shear and key Atlantic TC indices for various non-canonical El Niño definitions, i.e., CPW, EMI, TNI and PMM. One of the key points in our analyses is that, in order to isolate the impact of non-canonical El Niño, the influence of MDR SST is objectively removed from the Atlantic TC indices and MDR wind shear prior to making the composites by using the method of linear regression.

2. Data

[6] The SST dataset used in this study is the NOAA Extended Reconstructed Sea Surface Temperature version 3 (ERSST3) [*Smith et al.*, 2008] for the Atlantic hurricane season of June to November (JJASON) from the period of 1950–2010. The NCEP-NCAR Reanalysis-1 data for the same season and period is used to compute the wind shear and geopotential thickness between 200 and 850 hPa [*Kalnay et al.*, 1996]. The hurricane reanalysis database (HURDAT) from the National Hurricane Center for the same period is used to obtain various Atlantic TC indices.

[7] As discussed earlier, in order to isolate the impact of non-canonical El Niño patterns, the influence of MDR SST is removed from the Atlantic TC indices and wind shear by using the method of linear regression. For example, the modified MDR vertical wind shear (VWS) can be obtained by

$$\text{MDR VWS(modified)} = \text{MDR VWS} - a \times \text{MDR SSTA}, \quad (1)$$

where a ($= -1.96$ m s^{-1}°C^{-1}) is the regression coefficient of anomalous MDR SST onto the MDR wind shear (see Figure S1 in the auxiliary material).[1] All of our analyses in section 4 are performed both with and without this approach.

3. Indices for Non-canonical El Niño Patterns

[8] As pointed out by *Ashok et al.* [2007], the EOF2 of monthly tropical Pacific SST anomalies captures the distinct SST anomaly structure characteristic of the non-canonical El Niño. Various indices, such as CPW, EMI, TNI, and PMM have been suggested and used to define this same phenomenon. Currently, there is no consensus on how to classify the non-canonical El Niño. Hence, CPW, EMI, TNI and PMM are all reproduced for this study as described below. The referenced regions of SST anomalies are depicted in Figure S2 (and in Figure 1).

[9] *Ashok et al.* [2007] proposed EMI to determine non-canonical El Niño years. EMI is calculated using the following equation:

$$\text{EMI} = [\text{SSTA(A)} - 0.5 \times \text{SSTA(B)} - 0.5 \times \text{SSTA(C)}], \quad (2)$$

where SSTA(A) is the SST anomalies averaged over a box region for 10°S–10°N and 165°E–140°W, SSTA(B) is for 15°S–5°N and 110°W–70°W, and SSTA(C) is for 10°S–20°N and 125°E–145°E. In this study, the index is normalized ([ ] represents normalization) by the standard deviation of the EMI time series.

[10] *Yeh et al.* [2009] defined non-canonical El Niño years by establishing a set of criteria for what is called CPW. A CPW year occurs when warm SST anomaly in the Niño-4 region (NINO4; 5°S–5°N, 160°E–150°W) exceeds that of the Niño-3 region [*Yeh et al.*, 2009]. Note that CPW is not an index but rather criteria for handpicking non-canonical El Niño years, thus a CPW time series cannot be computed. CPW years are defined as those years in which NINO4 is greater than NINO3, while NINO4 is positive.

[11] *Chiang and Vimont* [2004] proposed PMM to describe an anomalous SST gradient across the mean latitude of the intertropical convergence zone (ITCZ) coupled to an anomalous displacement of the ITCZ toward the warmer region. PMM is calculated in this study using the following equation:

$$\text{PMM} = [[\text{ENP}] - [\text{NINO1} + 2]], \quad (3)$$

where ENP (eastern North Pacific) is the SST anomaly averaged over a box region for 10°N–30°N and 140°E–110°W, and NINO1 + 2 is the SST anomaly averaged over the Niño-1 + 2 region (10°S–0°N, 90°W–80°W). In this study, the index is normalized by the standard deviation of the PMM time series.

[12] *Trenberth and Stepaniak* [2001] suggested that an optimal characterization of both the distinct character and the evolution of each El Niño and La Niña event requires a so-called TNI in addition to the conventional SST anomalies in the Niño-3.4 region. TNI is computed by taking the difference between the normalized SST anomalies averaged in the Niño-1 + 2 and Niño-4 regions then further normalizing the resulting time series to have unit standard deviation. By normalizing the Niño-1 + 2 and Niño-4 SST anomaly terms prior to subtraction, neither region's SST anomaly can dominate the overall index. This is necessary because the magnitude of the equatorial eastern Pacific SST anomaly is usually larger than equatorial central Pacific SST anomaly. The resulting TNI is SST anomaly difference between the Niño-1 + 2 and Niño-4 regions. Note that *Trenberth and Stepaniak* [2001] calculate TNI by subtracting Niño-4 SST anomalies from Niño-1 + 2 SST anomalies so that a positive index corresponds to a cold central equatorial Pacific event. Here, in order for a positive TNI to correspond to a warmer

[1] Auxiliary materials are available in the HTML. doi:10.1029/2012GL052595.

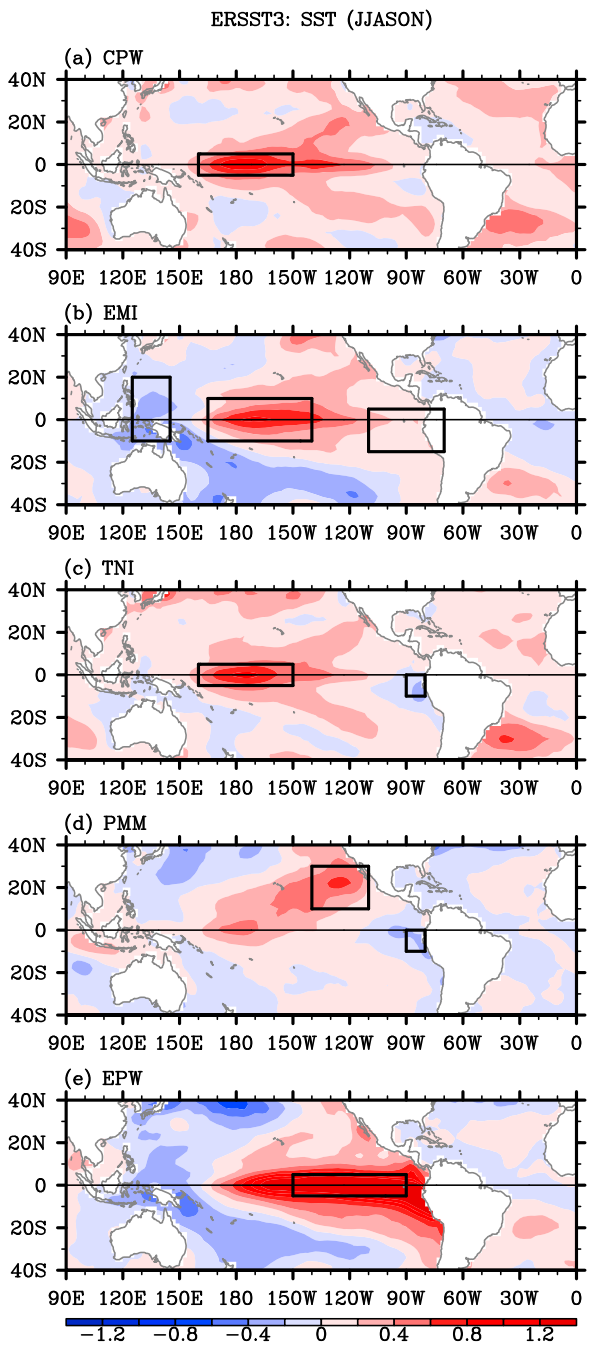

Figure 1. Composites of SST anomalies in JJASON for the eight strongest (+) phase (a) CPW, (b) EMI, (c) TNI, (d) PMM and (e) EPW years. The unit is °C. The black boxes indicate the SST regions referenced for the definitions of CPW (Niño-4), EMI (SSTA(A), SSTA(B), and SSTA(C)), TNI (Niño-4 and Niño-1 + 2), PMM (ENP and Niño-1 + 2) and EPW (Niño-3). See text for exact definitions of these SST regions.

than normal SST anomalies in the central tropical Pacific, the normalized Niño-1 + 2 SST anomalies are subtracted from the normalized Niño-4 SST anomalies in this study. Therefore, the equation for TNI is given by

$$\mathrm{TNI} = [[\mathrm{NINO4}] - [\mathrm{NINO1+2}]], \quad (4)$$

where [ ] represents that the variable is normalized.

[13] To represent each non-canonical El Niño definition, composites of the eight strongest positive (warm) phase years, during which NINO4 is also positive, are created for CPW, EMI, TNI and PMM. An additional criterion of NINO4 > 0 is required to eliminate years in which other regions' cold SST anomalies account for the positive index. For example, when calculating TNI, if NINO4 is 0 and NINO1 + 2 is negative, then TNI > 0. However, this is not a central tropical Pacific warming event but rather an eastern tropical Pacific cooling event. Therefore, including the criterion of NINO4 > 0 in selecting non-canonical El Niño years ensures that these types of years are discarded. NINO3 is also computed for the period 1950–2010 to create the composite of the eight strongest canonical El Niño years. Hereafter, NINO3 is also referred to as eastern Pacific warming (EPW). Note that each of these indices is first averaged for JJASON, and then is used in selecting the eight strongest positive phase years.

[14] Figure S3 displays the time series of EMI, TNI, PMM and EPW for JJASON during the period 1950–2010. EOF2 contains a strong low frequency signal, and is largely positive (i.e., warmer than normal in the central Pacific) during 1950–1970 and negative (i.e., colder than normal in the central Pacific) during 1997–2010 (not shown). EMI, TNI and PMM show more variability at the short time scales than EOF2. Overall, EMI and TNI agree in term of phase with the correlation coefficient of 0.86 (see Table S1). Similarly, TNI and PMM are significantly correlated with the correlation coefficient of 0.70, whereas EMI and EPW are poorly correlated with the correlation coefficient of 0.17.

4. Non-canonical El Niño Patterns and Atlantic TC Activity

[15] To quantify the impact of non-canonical El Niño on Atlantic TC activity, the number of tropical storms (TS), hurricanes (HR), major hurricanes (MH, categories 3–5), accumulated cyclone energy (ACE), number of United States landfalling hurricanes (USL), and the MDR wind shear for JJASON are averaged for each index's eight-year composite before and after removing the effect of Atlantic MDR SST (Table 1). For reference, the Atlantic TC indices and MDR wind shear for each of the eight strongest positive phase years for CPW, EMI, TNI, PMM, and EPW are shown in Table S2, S3, S4, S5, and S6, respectively.

[16] It is clear from Table 1 that only EPW shows all Atlantic TC indices (i.e., TS, HR, MH, ACE and USL) decreased and the MDR wind shear increased at the 90% significance level. Removing the effect of the Atlantic MDR SST has very minor impact (parenthesized values). In CPW and EMI, some Atlantic TC indices are decreased and the MDR wind shear is slightly increased before and after the Atlantic MDR SST impact is removed. However, these changes are too small to be statistically significant at the 90% level. In TNI, on the other hand, some Atlantic TC indices (i.e., TS, HR and ACE) are increased and the MDR wind shear is decreased before the Atlantic MDR SST impact is removed (non-parenthesized value). After the Atlantic MDR SST impact is removed (parenthesized value), however, all Atlantic TC indices and the MDR wind shear recover their climatological values. In PMM, all Atlantic TC indices are virtually indistinguishable from their climatological values. Removing the effect of the

Table 1. Atlantic TC Indices and MDR Vertical Wind Shear (VWS) Averaged for the Eight Strongest (+) Phase CPW, EMI, TNI, PMM and EPW Years Within the Period 1950–2010[a]

Index	TS (#)	HR (#)	MH (#)	ACE (10^4 kt^2)	USL (#)	VWS (m s^{-1})
CPW	11	6	2	97.0	2	0.3
	(11)	(6)	(2)	(91.3)	(2)	(0.4)
EMI	10	6	2	96.9	2	0.1
	(10)	(6)	(2)	(99.9)	(2)	(0.1)
TNI	14	8	3	120.1	2	−0.3
	(12)	(7)	(3)	(105.9)	(2)	(0.0)
PMM	11	7	3	103.3	1	0.2
	(11)	(7)	(3)	(104.0)	(1)	(0.2)
EPW	**8**	**3**	**1**	**53.6**	**1**	**1.4**
	(**8**)	(**3**)	(**1**)	(**51.7**)	(**1**)	(**1.5**)
Climatology	11	7	3	106.3	2	0.0

[a]Using HURDAT, the number of tropical storms (TS), hurricanes (HR), major hurricanes (MH, categories 3–5), accumulated cyclone energy (ACE), and number of United States landfalling hurricanes (USL) are averaged for each index's eight-year composite. For wind shear, the vertical wind shear (VWS) anomalies in June–November (JJASON) are averaged over the main development region (MDR, 85°W–15°W, 10°N–20°N) for each index's eight-year composite. The values in parenthesis are those after the influence of MDR SST is removed by using the method of linear regression. The regression coefficient ($a = -1.96$ m s^{-1}°C^{-1}) is above 99% significance level (see Figure S1). Any value larger or smaller than the climatological mean with above the 90% significance is in bold.

Atlantic MDR SST has no impact in this case (parenthesized values).

[17] In summary, in agreement with earlier studies [e.g., *Gray*, 1984; *Goldenberg and Shapiro*, 1996; *Kossin et al.*, 2010; *Klotzbach*, 2011], we find consistent evidence that the canonical El Niño suppresses Atlantic TC activity due to a large increase of the MDR wind shear. Some non-canonical El Niño patterns (CPW and EMI) also tend to slightly suppress Atlantic TC activity due to a weak-to-moderate increase of the MDR wind shear. However, their impact is insubstantial in comparison to that of the canonical El Niño. Therefore, here we do not find any evidence that links any of the four non-canonical El Niño patterns to Atlantic TC activity. This conclusion is also valid if Atlantic TC activity during the most active season of August–October (ASO) is considered (see Table S7).

5. Comparison With Earlier Studies

[18] *Kim et al.* [2009] and *Lee et al.* [2010] considered only five strongest CPW years, whereas this study uses eight strongest positive phase years for CPW (as well as for EMI, TNI and PMM). To test if our main conclusion is affected by the sample size, Table 1 is reproduced by using only the five strong positive phase years for each ENSO index (Table S8). As shown in the new table, the Atlantic TC indices and MDR wind shear are affected significantly (at the 90% significance level) only by the canonical El Niño (EPW), consistent with our main conclusion.

[19] It is also worthwhile to point out that *Kim et al.* [2009] identified the five strongest CPW years (1969, 1991, 1994, 2002, and 2004) based on linearly detrended tropical Pacific SSTs averaged for ASO. In this study, tropical Pacific SSTs (as well as tropical Atlantic SSTs) and Atlantic TC indices are not detrended and they are averaged for JJASON. Due to these differences, 1969 and 1991 were identified as CPW years in *Kim et al.* [2009], but they are not included in the list of eight strongest CPW years (see Table S2). Interestingly, 1991 is identified as a canonical El Niño year (Table S6). However, if tropical Pacific SSTs are averaged for ASO, 1991 is indeed identified as a strong CPW year. 1991 was a year of below normal Atlantic TC activity (see Tables S6 and S9). 1969, on the other hand, was a year of much increased Atlantic TC activity (Table S9). However, ASO of 1969 should be considered as a weak-to-moderate canonical El Niño season because NINO3 was only 0.63°C and greater than NINO4 (0.58°C).

6. Tropical Teleconnections Induced by Non-canonical El Niño Patterns

[20] Two key differences between the four non-canonical El Niño patterns and the canonical El Niño pattern are seen in the tropical Pacific SST anomaly distributions for JJASON (Figure 1). First, the maximum (warm) SST anomalies for the four non-canonical El Niño patterns are located in either the central tropical Pacific (EMI) or near the dateline (CPW, TNI and PMM), whereas those for the canonical El Niño are in the eastern tropical Pacific. But, more importantly, the amplitude of tropical Pacific SST anomalies associated with the non-canonical El Niño patterns is much weaker than that of the canonical El Niño. Consequently, the tropical tropospheric warming associated with the four non-canonical El Niño patterns is relatively weak and largely confined in the tropical Pacific region (Figures 2a–2d). EOF2 correlation map of temperature anomalies at 500 hPa shows a consistent result [see *Trenberth and Smith*, 2009, Figure 7]. In contrast, the tropical tropospheric warming associated with the canonical El Niño is much stronger, and its teleconnection to the tropical Atlantic region is clearly visible (Figure 2e). Therefore, we can conclude that the tropical Pacific SST anomalies associated with the non-canonical El Niño patterns are not strong enough to cause a substantial warming of the tropical troposphere in the Atlantic region, which is the key factor that increases the meridional tropospheric temperature gradient and atmospheric static stability over the MDR. Note that the meridional tropospheric temperature gradient over the tropical Atlantic has a direct influence on the MDR wind shear via the thermal wind relationship. The atmospheric static stability and associated anomalous diabatic heating (or cooling) over the MDR also influence the MDR wind shear via the formation of a stationary baroclinic Rossby wave northwest of the MDR [e.g., *Lee et al.*, 2011]. Therefore, consistent with the lack of teleconnected tropospheric warming over the tropical Atlantic in Figures 2a–2d, the MDR wind shear values for CPW, EMI, TNI and PMM are either neutral or only slightly increased (Figures 3a–3d).

7. Discussions

[21] The highlight of our major findings is that some non-canonical El Niño patterns tend to slightly suppress Atlantic TC activity due to a weak-to-moderate increase of the MDR wind shear. However, the overall impact of non-canonical El Niños is very small compared to that of the canonical El Niño. This result becomes more conclusive

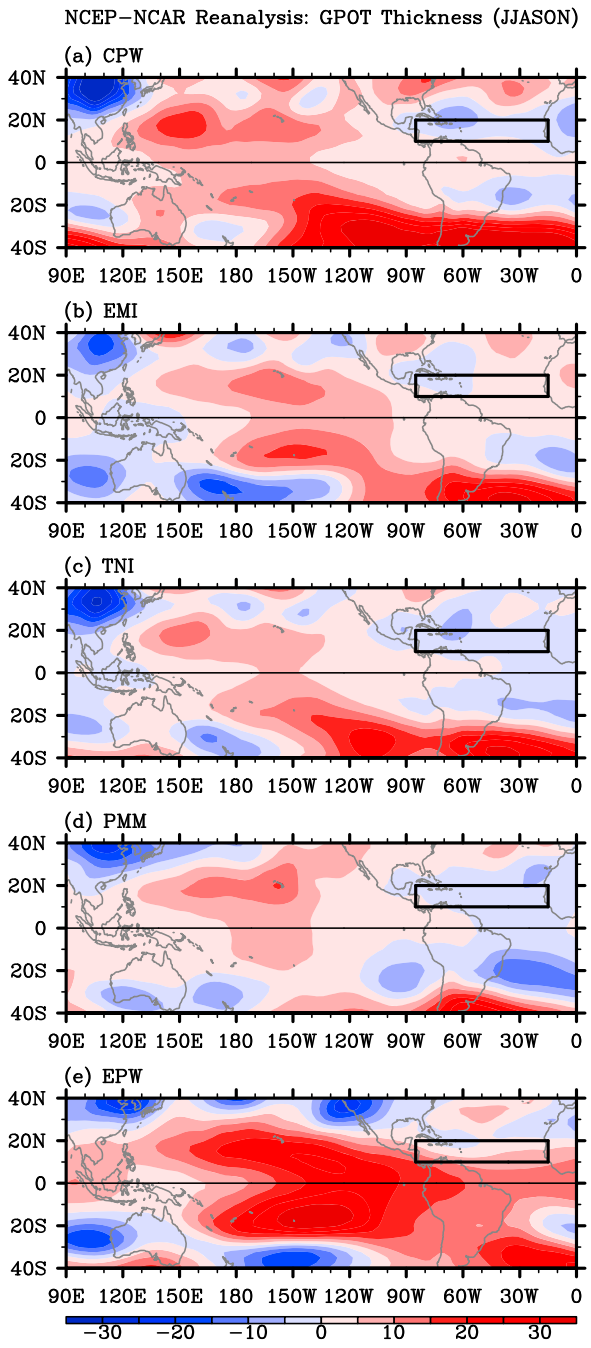

Figure 2. Composites of geopotential thickness (200 minus 850 hPa) anomalies in JJASON for the eight strongest (+) phase (a) CPW, (b) EMI, (c) TNI, (d) PMM and (e) EPW years. The influence of MDR SST is removed prior to making these composites by using the method of linear regression. The unit is gpm. The black box in each plot indicates the main development region (MDR, 85°W–15°W, 10°N–20°N).

when the effect of MDR SST is removed from the Atlantic TC indices and MDR wind shear.

[22] Recent studies reported that, during the recent decades, the non-canonical El Niños have been more frequent while the canonical El Niño has been less frequent [*Yeh et al.*, 2009; *Lee and McPhaden*, 2010]. *Yeh et al.* [2009] suggested that such trend may continue in the future due to anthropogenic greenhouse effect on the tropical Pacific thermocline. If this is indeed the case, an important implication is that the suppressing effect of El Niño on Atlantic TC activity may diminish and thus the MDR SST may play a more important role in controlling Atlantic TC activity in the coming decades.

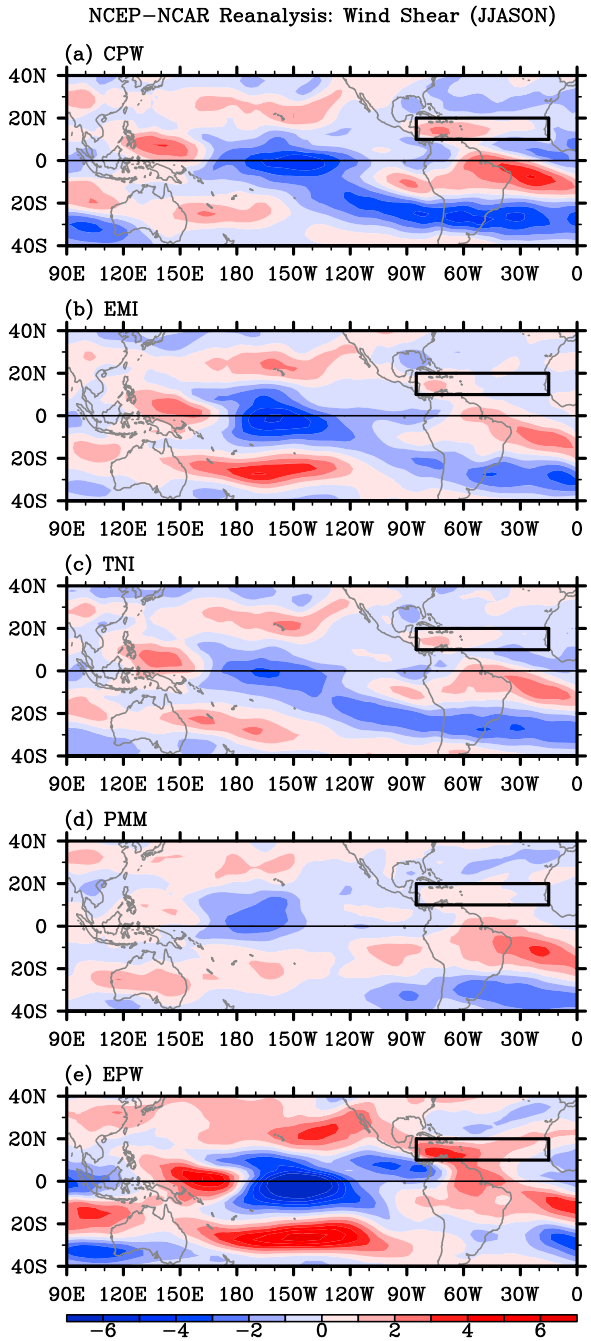

Figure 3. Composites of vertical wind shear (200 minus 850 hPa) anomalies in JJASON for the eight strongest (+) phase (a) CPW, (b) EMI, (c) TNI, (d) PMM and (e) EPW years. The influence of MDR SST is removed prior to making these composites by using the method of linear regression. The unit is m s^{-1}. The black box in each plot indicates the main development region (MDR, 85°W–15°W, 10°N–20°N).

[23] **Acknowledgments.** We wish to thank Jay Harris and Hailong Liu for their assistance in data acquisition and processing, and two anonymous reviewers and Greg Foltz for helpful comments and suggestions. This work was supported by the NOAA Ernest F. Hollings undergraduate scholarship program, and grants from the NOAA's Climate Program Office and the National Science Foundation.

[24] The Editor thanks two anonymous reviewers for assisting in the evaluation of this paper.

References

Ashok, K., S. Behera, A. S. Rao, H. Y. Weng, and T. Yamagata (2007), El Niño Modoki and its possible teleconnection, *J. Geophys. Res.*, *112*, C11007, doi:10.1029/2006JC003798.

Camargo, S. J., K. A. Emanuel, and A. H. Sobel (2007), Use of a genesis potential index to diagnose ENSO effects on tropical cyclone genesis, *J. Clim.*, *20*, 4819–4834, doi:10.1175/JCLI4282.1.

Chiang, J. C. H., and A. H. Sobel (2002), Tropical tropospheric temperature variations caused by ENSO and their influence on the remote tropical climate, *J. Clim.*, *15*, 2616–2631, doi:10.1175/1520-0442(2002)015<2616:TTTVCB>2.0.CO;2.

Chiang, J. C. H., and D. J. Vimont (2004), Analogous Pacific and Atlantic meridional modes of tropical atmosphere–ocean variability, *J. Clim.*, *17*, 4143–4158, doi:10.1175/JCLI4953.1.

Goldenberg, S. B., and L. J. Shapiro (1996), Physical mechanisms for the association of El Niño and West African rainfall with Atlantic major hurricane activity, *J. Clim.*, *9*, 1169–1187, doi:10.1175/1520-0442(1996)009<1169:PMFTAO>2.0.CO;2.

Gray, W. M. (1984), Atlantic seasonal hurricane frequency. Part I: El Niño and 30 mb Quasi-Biennial Oscillation influences, *Mon. Weather Rev.*, *112*, 1649–1668, doi:10.1175/1520-0493(1984)112<1649:ASHFPI>2.0.CO;2.

Horel, J. D., and J. M. Wallace (1981), Planetary-scale atmospheric phenomena associated with the Southern Oscillation, *Mon. Weather Rev.*, *109*, 813–829, doi:10.1175/1520-0493(1981)109<0813:PSAPAW>2.0.CO;2.

Kalnay, E., et al. (1996), The NCEP/NCAR 40-year reanalysis project, *Bull. Am. Meteorol. Soc.*, *77*, 437–471, doi:10.1175/1520-0477(1996)077<0437:TNYRP>2.0.CO;2.

Kao, H.-Y., and J.-Y. Yu (2009), Contrasting eastern-Pacific and central-Pacific types of ENSO, *J. Clim.*, *22*, 615–632, doi:10.1175/2008JCLI2309.1.

Kim, H.-M., P. J. Webster, and J. A. Curry (2009), Impact of shifting patterns of Pacific Ocean warming on North Atlantic tropical cyclones, *Science*, *325*, 77–80, doi:10.1126/science.1174062.

Klotzbach, P. J. (2011), El Niño–Southern Oscillation's impact on Atlantic basin hurricanes and U.S. landfalls, *J. Clim.*, *24*, 1252–1263, doi:10.1175/2010JCLI3799.1.

Knaff, J. A. (1997), Implications of summertime sea level pressure anomalies in the tropical Atlantic region, *J. Clim.*, *10*, 789–804, doi:10.1175/1520-0442(1997)010<0789:IOSSLP>2.0.CO;2.

Knight, J. R., C. K. Folland, and A. A. Scaife (2006), Climate impacts of the Atlantic multidecadal oscillation, *Geophys. Res. Lett.*, *33*, L17706, doi:10.1029/2006GL026242.

Kossin, J. P., and D. J. Vimont (2007), A more general framework for understanding Atlantic hurricane variability and trends, *Bull. Am. Meteorol. Soc.*, *88*, 1767–1781, doi:10.1175/BAMS-88-11-1767.

Kossin, J. P., S. J. Camargo, and M. Sitkowski (2010), Climate modulation of North Atlantic hurricane tracks, *J. Clim.*, *23*, 3057–3076, doi:10.1175/2010JCLI3497.1.

Kug, J.-S., F.-F. Jin, and S.-I. An (2009), Two types of El Niño events: Cold tongue El Niño and warm pool El Niño, *J. Clim.*, *22*, 1499–1515, doi:10.1175/2008JCLI2624.1.

Lee, T., and M. J. McPhaden (2010), Increasing intensity of El Niño in the central-equatorial Pacific, *Geophys. Res. Lett.*, *37*, L14603, doi:10.1029/2010GL044007.

Lee, S.-K., C. Wang, and D. B. Enfield (2010), On the impact of central Pacific warming events on Atlantic tropical storm activity, *Geophys. Res. Lett.*, *37*, L17702, doi:10.1029/2010GL044459.

Lee, S.-K., D. B. Enfield, and C. Wang (2011), Future impact of differential inter-basin ocean warming on Atlantic hurricanes, *J. Clim.*, *24*, 1264–1275, doi:10.1175/2010JCLI3883.1.

Saunders, M. A., and A. S. Lea (2008), Large contribution of sea surface warming to recent increase in Atlantic hurricane activity, *Nature*, *451*, 557–560, doi:10.1038/nature06422.

Smith, T. M., R. W. Reynolds, T. C. Peterson, and J. Lawrinmore (2008), Improvements to NOAA's historical merged land-ocean surface temperature analysis (1880–2006), *J. Clim.*, *21*, 2283–2296, doi:10.1175/2007JCLI2100.1.

Tang, B. H., and J. D. Neelin (2004), ENSO influence on Atlantic hurricanes via tropospheric warming, *Geophys. Res. Lett.*, *31*, L24204, doi:10.1029/2004GL021072.

Trenberth, K. E., and L. Smith (2009), Variations in the three dimensional structure of the atmospheric circulation with different flavors of El Niño, *J. Clim.*, *22*(11), 2978–2991, doi:10.1175/2008JCLI2691.1.

Trenberth, K. E., and D. P. Stepaniak (2001), Indices of El Niño evolution, *J. Clim.*, *14*, 1697–1701, doi:10.1175/1520-0442(2001)014<1697:LIOENO>2.0.CO;2.

Vimont, D. J., and J. P. Kossin (2007), The Atlantic meridional mode and hurricane activity, *Geophys. Res. Lett.*, *34*, L07709, doi:10.1029/2007GL029683.

Wang, C., D. B. Enfield, S.-K. Lee, and C. W. Landsea (2006), Influences of Atlantic warm pool on Western Hemisphere summer rainfall and Atlantic hurricanes, *J. Clim.*, *19*, 3011–3028, doi:10.1175/JCLI3770.1.

Yeh, S.-W., J.-S. Kug, B. Dewitte, M.-H. Kwon, B. Kirtman, and F.-F. Jin (2009), El Niño in a changing climate, *Nature*, *461*, 511–514, doi:10.1038/nature08316.

Yulaeva, E., and J. M. Wallace (1994), The signature of ENSO in global temperature and precipitation fields derived from the microwave sounding unit, *J. Clim.*, *7*, 1719–1736, doi:10.1175/1520-0442(1994)007<1719:TSOEIG>2.0.CO;2.

Zhang, R., and T. L. Delworth (2006), Impact of Atlantic multidecadal oscillations on India/Sahel rainfall and Atlantic hurricanes, *Geophys. Res. Lett.*, *33*, L17712, doi:10.1029/2006GL026267.

Table S1. Correlation coefficients between EMI, TNI, PMM and EPW (NINO3) for JJASON. The values in parenthesis are those for ASO. Correlation coefficients above the 95% significance based on student's t test are in bold.

	EMI	TNI	PMM	EPW
EMI	-	**0.86** (**0.87**)	**0.53** (**0.51**)	0.17 (0.23)
TNI	**0.86** (**0.87**)	-	**0.70** (**0.66**)	-0.14 (-0.07)
PMM	**0.53** (**0.51**)	**0.70** (**0.66**)	-	-0.42 -0.40
EPW	0.17 (0.23)	-0.14 (-0.07)	**-0.42** (**-0.40**)	-

Table S2. Hurricane indices for the eight strongest CPW years during 1950-2010. The number of tropical storms (TS), hurricanes (HR), major hurricanes (MH, categories 3-5), accumulated cyclone energy (ACE), and number of United States landfalling hurricanes (USL) obtained from HURDAT are shown. For wind shear, the vertical wind shear (VWS) anomalies in JJASON are averaged over the main development region (MDR, 85°W – 15°W, 10°N – 20°N). The values in parenthesis are those after the influence of MDR SST is removed by using the method of linear regression. The regression coefficient (a = -1.96 $m\ s^{-1}\ ^{o}C^{-1}$) is above 99% significance level (see Figure S1).

Year	NINO4	TS (#)	HR (#)	MH (#)	ACE ($10^4\ kt^2$)	USL(#)	VWS (ms^{-1})
2002	0.96	12 (12)	4 (4)	2 (2)	63.5 (57.1)	1 (1)	1.3 (1.4)
1994	0.89	7 (9)	3 (4)	0 (1)	28.8 (50.8)	0 (0)	0.0 (-0.5)
2004	0.88	15 (12)	9 (7)	6 (5)	227.3 (183.9)	6 (6)	-1.0 (-0.1)
2003	0.57	16 (13)	7 (5)	3 (2)	180.3 (143.8)	2 (2)	-0.5 (0.3)
1986	0.48	6 (9)	4 (6)	0 (1)	41.4 (75.8)	2 (2)	2.1 (1.4)
2001	0.46	15 (13)	9 (8)	4 (3)	115.6 (91.6)	0 (0)	-0.3 (0.2)
1990	0.45	14 (13)	8 (7)	1 (1)	93.0 (76.3)	0 (0)	-0.3 (0.1)
1977	0.44	6 (8)	5 (6)	1 (2)	26.5 (50.8)	1 (1)	1.0 (0.5)
Climatology	0.00	11	7	3	106.3	2	0.0

Table S3. Same as Table S2, but for the eight strongest positive EMI years during 1950-2010.

Year	EMI	TS (#)	HR (#)	MH (#)	ACE (10^4 kt^2)	USL(#)	VWS (ms^{-1})
1994	1.50	7 (9)	3 (4)	0 (1)	28.8 (50.8)	0 (0)	0.0 (-0.5)
1966	1.38	11 (11)	7 (7)	3 (3)	148.9 (146.3)	2 (2)	-0.9 (-0.9)
2004	1.24	15 (12)	9 (7)	6 (5)	227.3 (183.9)	6 (6)	-1.0 (-0.1)
1990	1.10	14 (13)	8 (7)	1 (1)	93.0 (76.3)	0 (0)	-0.3 (0.1)
1977	1.05	6 (8)	5 (6)	1 (2)	26.5 (50.8)	1 (1)	1.0 (0.5)
1991	1.04	8 (10)	4 (5)	2 (3)	39.2 (63.6)	1 (1)	1.6 (1.0)
1958	0.75	10 (8)	7 (6)	5 (4)	127.2 (100.1)	1 (1)	-0.3 (-0.3)
1965	0.74	6 (8)	4 (5)	1 (2)	84.3 (111.3)	1 (1)	0.6 (0.1)
Climatology	0.00	11	7	3	106.3	2	0.0

Table S4. Same as Table S2, but for the eight strongest positive TNI years during 1950-2010.

Year	TNI	TS (#)	HR (#)	MH (#)	ACE (10^4 kt^2)	USL(#)	VWS (ms^{-1})
1994	1.44	7 (9)	3 (4)	0 (1)	28.8 (50.8)	0 (0)	0.0 (-0.5)
2001	1.33	15 (13)	9 (8)	4 (3)	115.6 (91.6)	0 (0)	-0.3 (0.2)
2004	1.23	15 (12)	9 (7)	6 (5)	227.3 (183.9)	6 (6)	-1.0 (-0.1)
1977	1.09	6 (8)	5 (6)	1 (2)	26.5 (50.8)	1 (1)	1.0 (0.5)
1966	1.04	11 (11)	7 (7)	3 (3)	148.9 (146.3)	2 (2)	-0.9 (-0.9)
2005	1.03	28 (23)	15 (12)	7 (5)	257.5 (189.7)	6 (6)	-2.2 (-0.7)
1990	1.01	14 (13)	8 (7)	1 (1)	93.0 (76.3)	0 (0)	-0.3 (0.1)
2002	0.98	12 (12)	4 (4)	2 (2)	63.5 (57.1)	1 (1)	1.3 (1.4)
Climatology	0.00	11	7	3	106.3	2	0.0

Table S5. Same as Table S2, but for the eight strongest positive PMM years during 1950-2010.

Year	PMM	TS (#)	HR (#)	MH (#)	ACE (10^4 kt^2)	USL(#)	VWS (ms^{-1})
1992	1.39	7 (8)	4 (5)	1 (1)	77.3 (92.3)	1 (1)	0.7 (0.3)
1990	1.23	14 (13)	8 (7)	1 (1)	93.0 (76.3)	0 (0)	-0.3 (0.1)
1996	1.12	13 (13)	9 (9)	6 (6)	177.2 (180.0)	2 (2)	0.8 (0.7)
1958	0.94	10 (8)	7 (6)	5 (4)	127.2 (100.1)	1 (1)	-0.3 (-0.3)
2001	0.89	15 (13)	9 (8)	4 (3)	115.6 (91.6)	0 (0)	-0.3 (0.2)
1968	0.72	8 (9)	4 (5)	0 (7)	45.9 (69.7)	1 (1)	-0.2 (-0.8)
1986	0.68	6 (9)	4 (6)	0 (1)	41.4 (75.8)	2 (2)	2.1 (1.4)
1966	0.67	11 (11)	7 (7)	3 (3)	148.9 (146.3)	2 (2)	-0.9 (-0.9)
Climatology	0.00	11	7	3	106.3	2	0.0

Table S6. Same as Table S2, but for the eight strongest canonical El Niño (EPW) years during 1950-2010.

Year	NINO3	TS (#)	HR (#)	MH (#)	ACE (10^4 kt^2)	USL(#)	VWS (ms^{-1})
1997	2.78	8 (6)	3 (2)	1 (0)	41.4 (19.6)	1 (1)	0.2 (0.7)
1972	1.71	7 (10)	3 (5)	0 (1)	36.7 (70.0)	1 (1)	3.4 (2.7)
1982	1.67	6 (8)	2 (3)	1 (2)	31.5 (55.5)	0 (0)	2.7 (2.1)
1987	1.41	7 (4)	3 (1)	1 (0)	30.2 (0.0)	1 (1)	1.3 (2.1)
1965	1.21	6 (8)	4 (5)	1 (2)	84.3 (111.3)	1 (1)	0.6 (0.1)
1957	1.08	8 (8)	3 (3)	2 (2)	86.8 (84.9)	1 (1)	-0.2 (-0.2)
2009	0.96	9 (6)	3 (2)	2 (1)	54.6 (22.0)	0 (0)	2.1 (2.8)
1991	0.89	8 (10)	4 (5)	2 (3)	39.2 (63.6)	1 (1)	1.6 (1.1)
Climatology	0.00	11	7	3	106.3	2	0.0

Table S7. Same as Table 1, but only for August-October (ASO).

Index	TS (#)	HR (#)	MH (#)	ACE (10^4 kt^2)	USL(#)	VWS (ms^{-1})
CPW	9 (8)	5 (4)	2 (2)	86.5 (75.9)	1 (1)	0.1 (0.4)
EMI	8 (8)	5 (5)	2 (2)	81.9 (81.7)	0 (0)	0.0 (0.0)
TNI	10 (9)	6 (5)	3 (2)	95.4 (82.0)	2 (1)	-0.2 (0.1)
PMM	10 (9)	6 (6)	3 (3)	115.9 (102.1)	1 (1)	-0.2 (0.2)
EPW	**6** (**6**)	**3** (**3**)	**1** (**1**)	**50.0** (**49.4**)	**0** (**0**)	**0.9** (**0.9**)
Climatology	8	5	3	93.3	1	0.0

Table S8. Same as Table 1, but by using only the five strongest (+) phase years.

Index	TS (#)	HR (#)	MH (#)	ACE (10^4 kt^2)	USL(#)	VWS (ms^{-1})
CPW	11 (11)	5 (5)	2 (2)	108.5 (102.3)	2 (2)	0.4 (0.5)
EMI	11 (10)	6 (6)	2 (2)	104.9 (101.6)	2 (2)	-0.2 (-0.2)
TNI	11 (10)	7 (6)	3 (3)	109.4 (104.7)	2 (2)	-0.3 (-0.2)
PMM	12 (11)	7 (7)	3 (3)	118.0 (108.1)	1 (1)	0.1 (**0.3**)
EPW	**7** (**7**)	**3** (**3**)	**1** (**1**)	**44.8** (**50.0**)	**1** (**1**)	**1.6** (**1.5**)
Climatology	8	5	3	93.3	1	0.0

Table S9. Same as Table S2, but for the five CPW years considered in Kim et al. [2009] and Lee et al. [2010]. All indices in this table are averaged for August-October (ASO).

Year	NINO4	TS (#)	HR (#)	MH (#)	ACE (10^4 kt^2)	USL(#)	VWS (ms^{-1})
2004	1.00	13 (10)	8 (6)	5 (4)	214.4 (167.7)	5 (5)	-1.2 (0.1)
1994	0.94	4 (6)	1 (2)	0 (1)	10.0 (31.1)	0 (0)	0.0 (-0.6)
2002	0.94	11 (10)	4 (4)	2 (2)	61.0 (49.7)	1 (1)	1.6 (2.0)
1991	0.79	7 (8)	4 (5)	2 (2)	38.0 (53.8)	1 (1)	0.6 (0.1)
1969	0.58	16 (15)	11 (10)	5 (5)	155.9 (143.0)	2 (2)	-0.4 (0.0)
Mean	0.85	10 (10)	6 (5)	3 (3)	95.9 (89.1)	2 (2)	0.1 (0.3)
Climatology	0.00	8	5	3	93.3	1	0.0

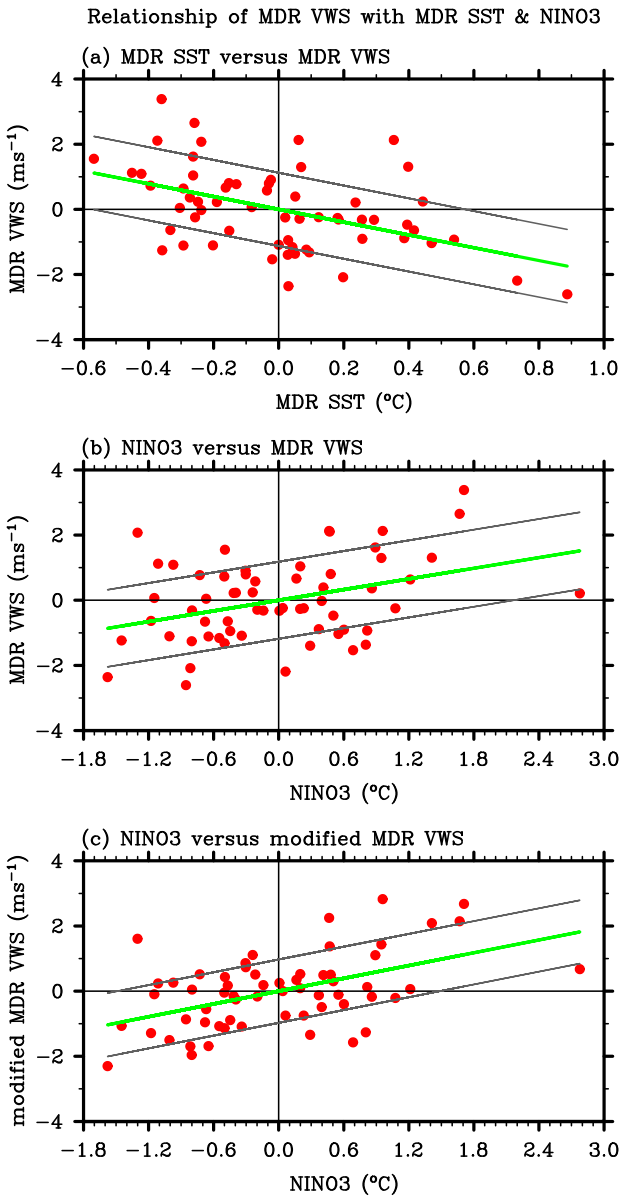

Figure S1. Scatterplot of (a) MDR SST versus MDR vertical wind shear (VWS), (b) NINO3 versus MDR VWS, and (c) NINO3 versus modified MDR VWS. All indices are those averaged for JJASON. The influence of MDR SST is removed in the modified MDR VWS by using the method of linear regression. For each plot, the green line is the linear regression, whereas the two gray lines show the standard error of the linear regression. The slope of the regression line is -1.96, 0.55, and 0.65 for (a), (b) and (c), respectively. All three linear regression lines are above the 99% significance level.

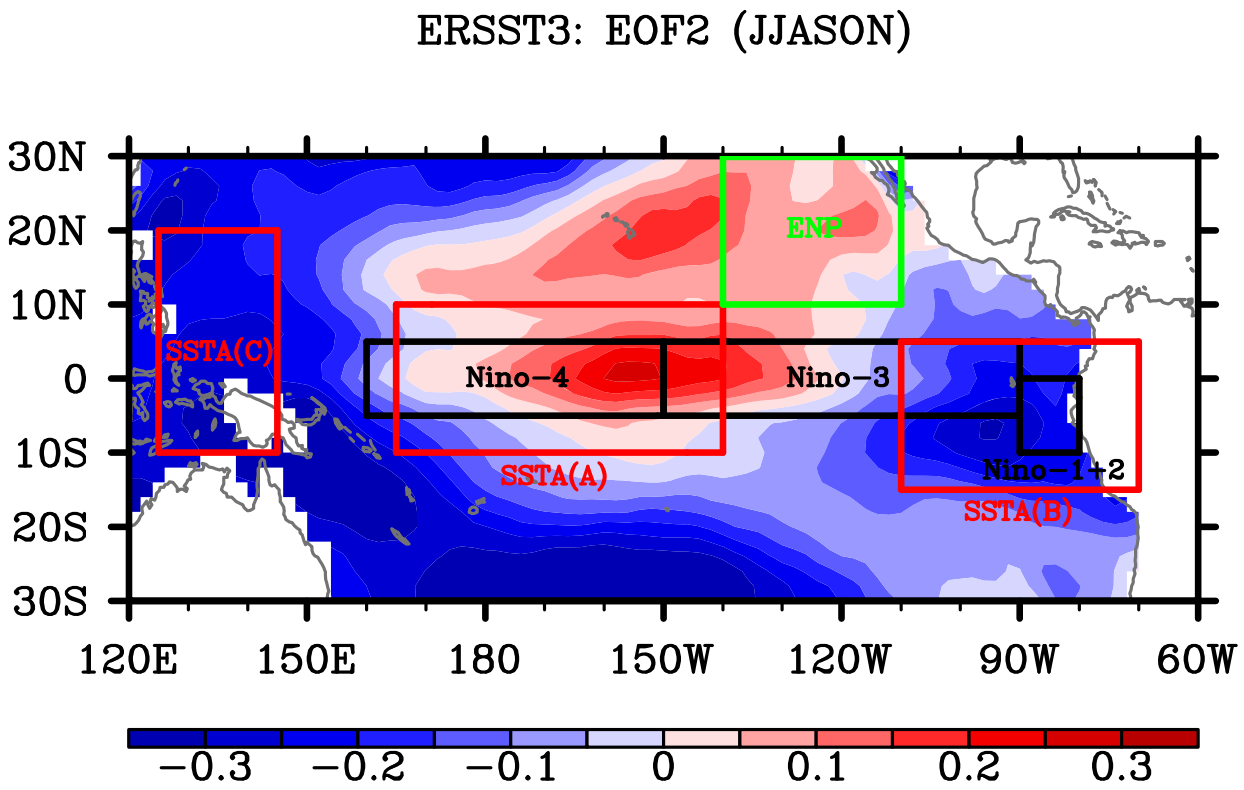

Figure S2. SST regions referenced for the definitions of four non-canonical El Niño patterns. See text for exact definitions of these SST regions. The background is the 2nd mode of the empirical orthogonal function (EOF2) analysis of the tropical Pacific SST anomalies. It is constructed by regressing the normalized EOF2 time series onto SST anomalies then averaging the regression coefficients for JJASON.

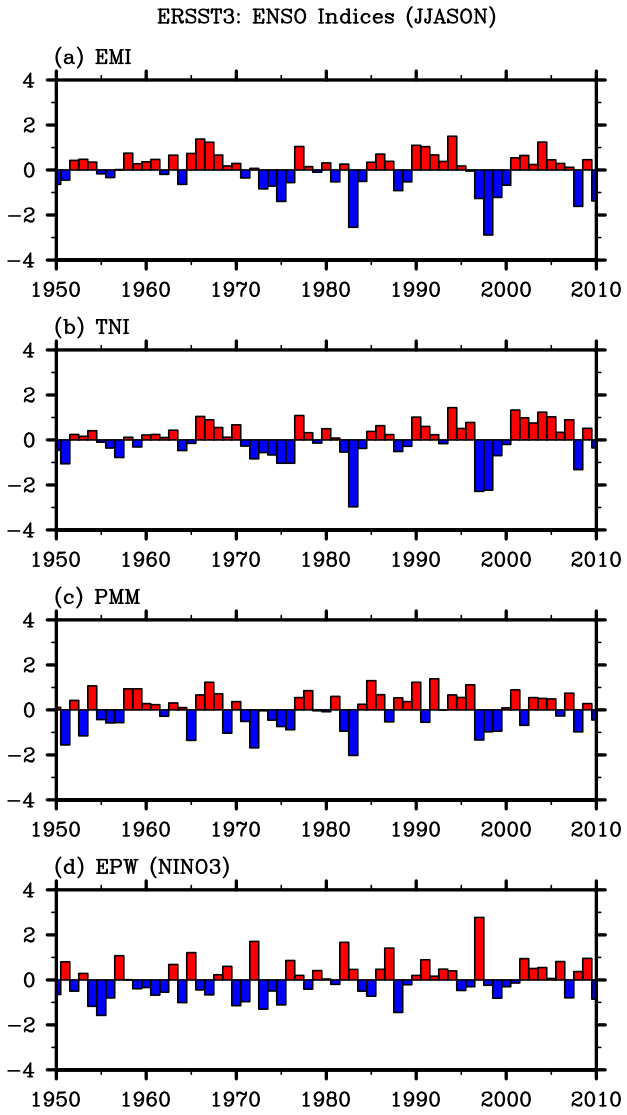

Figure S3. Time series of four non-canonical El Niño indices and the canonical El Niño (NINO3) index for JJASON during the period of 1950 - 2010. Each of the four non-canonical El Niño index is normalized by the standard deviation.